Binuclear platinum(II) complexes containing 1,1,4,7,10,10-hexaphenyl-1,4,7,10-tetraphosphadecane (P4): first X-ray structure of a tetraphos dimer

Hans Goller and Peter Brüggeller*

Institut für Anorganische und Analytische Chemie, Universität Innsbruck, Innrain 52a, 6020 Innsbruck (Austria)

(Received February 3, 1992; revised April 22, 1992)

Abstract

Several binuclear Pt(II) complexes containing 1,1,4,7,10,10-hexaphenyl-1,4,7,10-tetraphosphadecane (tetraphos-1, P4) have been prepared and characterized by $^{31}P\{^1H\}$ NMR spectroscopy, elemental analyses, melting points and an X-ray structure analysis. In the first steps of the syntheses complexes of the general formula *rac*- or *meso*-$[Pt_2Cl_3P4]X$ ($X = Cl^-$, (BF_4^-), (BPh_4^-)) (**1–6**) showing a *cis* P4 arrangement are formed. Transformation to thermodynamically more stable compounds (**1a–6a**) leads to the incorporation of the chloride anion in *cis,rac*- or *cis,meso*-$[Pt_2Cl_4P4]$ (**1a**, **2a**). The X-ray structure of **1a**, which is the first structure of a tetraphos dimer, has been determined (tetragonal, $P\bar{4}2_1c$; $a = 17.257(2)$, $c = 16.048(3)$ Å, $R = 0.048$ for 1107 observed reflections ($F > 6.0\ \sigma(F)$). It shows an open-mode dimer with a Pt–Pt distance of 6.338(1) Å and a *cis* P4 configuration. In the presence of non-coordinating anions a rearrangement of P4 from *cis* to *trans* occurs (**3a–6a**). The observation that P4 is able to coordinate two metal centers in a *cis* as well as in a *trans* manner is unusual for binuclear oligophosphine complexes.

Introduction

There is current interest in Pt(II) oligomers [1, 2]. This is partly due to their possible application in homogeneous catalysis [3]. A variable metal–metal distance is of great importance [4]. 1,1,4,7,10,10-Hexaphenyl-1,4,7,10-tetraphosphadecane (tetraphos-1, P4) has been shown to be a very flexible ligand in monometallic Pt(II) complexes [5, 6]. There have also been numerous cases of its oligometallic coordination behavior [7]. Here the syntheses of binuclear Pt(II) species with different structural features are presented. The X-ray structure of *cis,rac*-$[Pt_2Cl_4P4]$ (**1a**), which is the first structure of a tetraphos dimer, is given and the influence of non-coordinating anions X in $[Pt_2Cl_3P4]X$ complexes on their coordination geometries is studied.

Experimental

Reagents and chemicals

Reagent grade chemicals were used as received unless stated otherwise. 1,1,4,7,10,10-Hexaphenyl-1,4,7,10-tetraphosphadecane (P4) was purchased from Strem Chemical Co. $Na(BPh_4)$ was of purissimum grade quality and was received from Merck-Schuchardt. $Na(BF_4)$ and all organic solvents were obtained from Fluka. Solvents used for NMR measurements and crystallization purposes were of purissimum grade quality. $Na_2PtCl_4 \cdot 4H_2O$ was received from Fluka.

Instrumentation

Fourier-mode $^{31}P\{^1H\}$ NMR spectra were obtained by use of Bruker WP-80 (internal deuterium lock) and Bruker AM-300 (external deuterium lock) spectrometers and were recorded at 17.2 and 121.5 MHz, respectively. Positive chemical shifts are downfield from 85% H_3PO_4 used as standard.

X-ray data collection

The X-ray data collection was performed on a Siemens R3m/V diffractometer. Colorless crystals of *cis,rac*-$[Pt_2Cl_4P4]$ (**1a**) were sealed into a capillary. The lattice was found to be tetragonal by standard procedures using the software of the Siemens R3m/V diffractometer. No decay in the intensities of three standard reflections was observed during the course of data collection. The data were corrected for Lorentz and polarization effects. The empirical absorption correction was based on ψ-scans of nine reflections [8].

*Author to whom correspondence should be addressed.

0020-1693/92/$5.00

Solution and refinement of the structure

All structure determination calculations were done on a 80386-PC using the PC-version of SHELXTL PLUS [9]. The position of the platinum atom was found by direct methods. Other atoms positions were located from successive difference Fourier maps. One molecule acetonitrile per unit cell was included in the isotropic refinement. The phenyl rings have been refined as groups. Final refinement was carried out with anisotropic thermal parameters for all other non-hydrogen atoms. Hydrogen atoms were included using a riding model with fixed isotropic U. The final R value of 0.048 was computed for 113 parameters and 1107 reflections. The largest feature on a final difference map was 1.13 e A^{-3}. The largest shift/error in the final cycle of refinement was 0.001. The structure determination is summarized in Table 1. Table 2 shows positional parameters for *cis,rac*-[Pt_2Cl_4P4] (**1a**).

Separation of the stereoisomers of P4

Commercial P4 was separated by fractional crystallization to give the pure *rac* and *meso* diastereomer, respectively, according to Brown and Canning [7].

TABLE 1. Structure determination summary for *cis,rac*-[Pt_2Cl_4P4] (**1a**)

Formula	$C_{42}H_{42}Cl_4P4Pt_2 \cdot 0.25C_2H_3N$
Formula weight	1212.9
Color and habit	colorless; irregular
Crystal system	tetragonal
Space group	$P\bar{4}2_1c$
a (Å)	17.257(2)
c (Å)	16.048(3)
V (Å^3)	4779.16
T (K)	299
Z	4
Crystal dimensions (mm)	0.2×0.2×0.5
D_{calc} (Mg/m^3)	1.686
Radiation (Å)	Cu Kα (λ = 1.54184)
μ (mm^{-1})	6.29
F(000)	2331
Range of transmission factors	0.45–0.72
Diffractometer	Siemens R3m/V
Monochromator	Highly oriented graphite crystal
Scan type	2θ–θ
Scan speed (°/min)	Variable; 4.19 to 29.29 in ω
2θ Range (°)	3.0 to 115.0
Index ranges	$0<h<13$, $0<k<18$, $0<l<17$
Reflections collected	3539
Independent reflections	1817 (R_{int} = 0.038)
Observed reflections	1107 ($F>6.0\ \sigma(F)$)
No. parameters refined	113
Final R indices (observed data)	
R	0.048
R_w[a]	0.057
Goodness-of-fit	0.89
Largest and mean Δ/σ	0.001, 0.0005
Largest difference peak (e Å^{-3})	1.13
Largest difference hole (e Å^{-3})	−0.72

[a] $w^{-1} = \sigma^2(F) + 0.0010F^2$.

TABLE 2. Atomic coordinates (×10^4) and equivalent isotropic displacement coefficients (Å^2×10^3)

	x	y	z	U_{eq}[a]
Pt	6304(1)	1293(1)	141(1)	36(1)
Cl(1)	5431(5)	1136(6)	−968(4)	64(3)
Cl(2)	7369(4)	1300(5)	−780(4)	50(2)
P(1)	5318(4)	1245(5)	1019(4)	35(2)
P(2)	7056(4)	1397(5)	1259(4)	38(3)
C(1)	5650(15)	1299(17)	2090(16)	50(11)
C(2)	6459(13)	1734(14)	2119(16)	36(9)
C(3)	4826(17)	334(14)	987(18)	45(10)
C(11)	3956(13)	2022(12)	1376(12)	91(12)
C(12)	3429	2632	1313	106(15)
C(13)	3612	3284	837	81(11)
C(14)	4322	3325	425	126(17)
C(15)	4850	2716	489	77(11)
C(16)	4667	2064	964	33(6)
C(21)	7756(9)	2824(12)	1052(13)	81(10)
C(22)	8370	3348	997	72(9)
C(23)	9128	3094	1121	71(10)
C(24)	9274	2316	1299	97(13)
C(25)	8660	1792	1354	84(11)
C(26)	7901	2046	1230	43(7)
C(31)	7589(12)	290(12)	2395(11)	77(10)
C(32)	7887	−429	2631	96(13)
C(33)	8035	−993	2029	105(14)
C(34)	7885	−838	1191	85(13)
C(35)	7586	−119	955	81(12)
C(36)	7438	445	1557	28(6)
C(8)	0	0	603(72)	324(63)
N(8)	0	0	603(72)	324(63)
C(9)	0	0	0	247(92)

[a] Equivalent isotropic U defined as one third of the trace of the orthogonalized U_{ij} tensor.

Syntheses of Pt(II) complexes

A Schlenk apparatus and oxygen-free, dry Ar were used in the syntheses of all complexes. Solvents were degassed by several freeze–pump–thaw cycles prior to use. All reactions were carried out at room temperature unless stated otherwise.

*cis,rac-[Pt_2Cl_4P4] (**1a**) and cis,meso-[Pt_2Cl_4P4] (**2a**)*

To $Na_2PtCl_4 \cdot 4H_2O$ (0.3 mmol, 0.115 g) in water a solution of *rac* or *meso* P4 (0.15 mmol, 0.101 g) in CH_2Cl_2 was added. Then EtOH was added under stirring until a pale brown precipitate formed. **1** or **2** was filtered off, washed with water, and dried *in vacuo*: yields 0.166 g (81%) (**1**), 0.135 g (75%) (**2**); m.p. = 225 °C dec. (**1**), 170 °C dec. (**2**). *Anal.* Calc. for $C_{42}H_{42}Cl_4P4Pt_2$: C, 42.0; H, 3.5. Found: C, 41.7; H, 3.8 (**1**); C, 41.9; H, 3.7% (**2**).

A solution of **1** or **2** (0.1 mmol, 0.120 g) in CH_2Cl_2/MeOH (1:1) was stirred at 30 °C for 24 h. The solution was evaporated to dryness and the white residue recrystallized from CH_2Cl_2/MeOH/CH_3CN (1:1:1). **1a** and **2a**: colorless crystals, yield 0.110 g (92%) (**1a**), 0.105

g (87.5%) (**2a**); m.p. = 180–185 °C (**1a**), 150–155 °C (**2a**). *Anal.* Calc. for $C_{42}H_{42}Cl_4P4Pt_2 \cdot 0.25C_3H_3N$: C, 42.1; H, 3.6. Found: C, 42.2; H, 3.7 (**1a**); C, 42.4; H, 3.9% (**2a**).

rac-[Pt_2Cl_2(μ-Cl)P4](BF_4) (3a) and trans,meso-[Pt_2Cl_2(μ-Cl)P4](BF_4) (4a)

To $Na_2PtCl_4 \cdot 4H_2O$ (0.4 mmol, 0.153 g) and Na(BF_4) (0.4 mmol, 0.064 g) in water a solution of *rac* or *meso* P4 (0.2 mmol, 0.135 g) in CH_2Cl_2 was added. Then EtOH was added under stirring until a pale brown precipitate formed. **3** or **4** was filtered off, washed with water, and dried *in vacuo*: yields 0.188 g (75%) (**3**), 0.183 g (73%) (**4**); m.p. = 230–235 °C dec. (**3**), > 315 °C (**4**). *Anal.* Calc. for $C_{42}H_{42}BCl_3F_4P4Pt_2$: C, 40.2; H, 3.4. Found: C, 39.9; H, 3.6 (**3**); C, 40.0; H, 3.5% (**4**).

A solution of **3** or **4** (0.1 mmol, 0.125 g) in $MeNO_2$/MeOH/CH_2Cl_2 (2:1:1) was stirred at 35 °C for 48 h. The solution was evaporated to dryness and the white residue recrystallized from $MeNO_2$/MeOH/CH_2Cl_2. **3a** and **4a**: colorless crystals, yield 0.105 g (84%) (**3a**), 0.101 g (81%) (**4a**); m.p. = 310 °C dec. (**3a**), > 320 °C (**4a**). *Anal.* Calc. for $C_{42}H_{42}BCl_3F_4P4Pt_2$: C, 40.2; H, 3.4. Found: C, 39.8; H, 3.7 (**3a**); C, 40.1; H, 3.6% (**4a**).

trans,rac-[Pt_2Cl_2(μ-Cl)P4](BPh_4) (5a) and trans,meso-[Pt_2Cl_2(μ-Cl)P4](BPh_4) (6a)

To $Na_2PtCl_4 \cdot 4H_2O$ (0.4 mmol, 0.153 g) and Na(BPh_4) (0.4 mmol, 0.137 g) in water a solution of *rac* or *meso* P4 (0.2 mmol, 0.135 g) in CH_2Cl_2 was added. Then EtOH was added under stirring until a pale brown precipitate formed. **5** or **6** was filtered off, washed with water, and dried *in vacuo*: yields 0.217 g (73%) (**5**), 0.208 g (70%) (**6**); m.p. = 123–125 °C dec. (**5**), 115–117 °C dec. (**6**). *Anal.* Calc. for $C_{66}H_{62}BCl_3P4Pt_2$: C, 53.3; H, 4.2. Found: C, 53.0; H, 4.4 (**5**); C, 53.1; H, 4.5% (**6**).

A solution of **5** or **6** (0.1 mmol, 0.149 g) in EtOH/CH_2Cl_2 (2:1) was stirred at room temperature for 24 h. The solution was evaporated to dryness and the white residue recrystallized from CH_2Cl_2/$MeNO_2$ (3:2). **5a** and **6a**: colorless crystals, yield 0.112 g (75%) (**5a**), 0.109 g (73%) (**6a**); m.p. = 240 °C (**5a**), 158 °C dec. (**6a**). *Anal.* Calc. for $C_{66}H_{62}BCl_3P4Pt_2$: C, 53.3; H, 4.2. Found: C, 53.1; H, 4.5 (**5a**); C, 53.0; H, 4.4% (**6a**).

Results

The complexes **1–6** and **1a–6a** have been characterized by $^{31}P\{^1H\}$ NMR spectroscopy, elemental analyses, melting points and an X-ray structure analysis (*cis,rac*-[Pt_2Cl_4P4], **1a**). The compounds **1–6** are kinetically controlled and stable only in the solid state. In solution they slowly transform to the thermodynamically more stable complexes **1a–6a**. The ^{31}P NMR parameters of **1–6** (see Table 3) are in agreement with A_2B_2 spin systems and a *cis* P4 arrangement, where all four phosphorus atoms of P4 coordinate in a *cis* manner (see Scheme 1). Since a 1,2 *cis* structure type contains both the PPh as well as the PPh_2 groups as part of one five-ring a similar shift is expected for the two groups [10] (see Table 3). The comparable small ^1J(Pt, P) values are in agreement with the presence of a P–Pt–Pt–Cl structural unit [11]. Therefore a [Pt(Cl)–Pt(Cl)$_2$P4]X (X = anion) structure is tentatively assumed containing a four- and a five-coordinate platinum(II) center connected by dynamic averaging. The presence of a dynamic process is confirmed by the broadness of the ^{31}P NMR signals showing no resolved ^2J(Pt, P) couplings.

However, the Pt–Pt bond is labile and in solution a chloro bridge is slowly formed leading in the cases of **1** and **2** to *cis*-[Pt_2Cl_2(μ-Cl)P4]Cl (structure type A in Scheme 2). This process leads to an enhancement of the ^1J(Pt, P) values by about 1500 Hz due to the low *trans* influence of chloride [11, 12]. The chloro bridges are indicated by ^3J(Pt, PPh) couplings in the typical range [13] (*rac*: 54 Hz, *meso*: 64 Hz). However, in *cis*-[Pt_2Cl_2(μ-Cl)P4]Cl an incorporation of the chloride anion leading to *cis*-[Pt_2Cl_4P4] (**1a**, **2a**) is possible as a next step (structure type B in Scheme 2).

In order to characterize *cis,rac*-[Pt_2Cl_4P4] (**1a**) definitely, the solid state structure was determined by X-ray crystallography. It shows that the incorporation of the chloride anion during transformation has occurred. A view of *cis,rac*-[Pt_2Cl_4P4] (**1a**) is given in Fig. 1. Table 4 contains selected bond distances and bond angles.

This represents the first X-ray structure on a bimetallic tetraphos complex. It consists of discrete *cis,rac*-[Pt_2Cl_4P4] molecules and one molecule CH_3CN per unit cell. *cis,rac*-[Pt_2Cl_4P4] is located on a two-fold symmetry axis. The square-planar coordinations of the platinum atoms in *cis,rac*-[Pt_2Cl_4P4] are only slightly distorted. The deviations are mainly a consequence of the two chelate five-rings constraining the P–Pt–P angles to 86.5(3)°. This results in an opening of the Cl–Pt–Cl and one pair of the Cl–Pt–P angles to 91.5(2) and

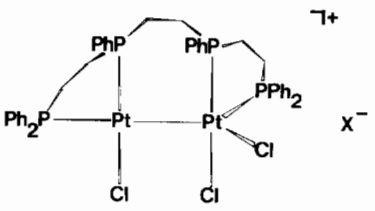

Scheme 1. Structure type observed in the dimers **1–6**. The P–Pt–P angles where the phosphorus atoms are connected by ethylene chains are constrained to about 85°.

TABLE 3. $^{31}P\{^1H\}$ NMR data for **1–6** and **1a–6a**[a]

Compound	δPPh	δPPh$_2$	^1J(Pt, PPh)	^1J(Pt, PPh$_2$)
1	42.6		1960	
2	38.3		2230	
3	46.2	43.3	2322	2300
4	43.5	38.7	2750	2457
5	30.8, 29.9	−1.5	2034, 2028	688
6	42.4		1804	
1a	45.8	41.6	3588	3630
2a	50.0	42.5	3591	3613
3a	82.6, 44.0[b]	39.5, 11.2	3086, 1299	2069, 2556
	(30)	(43)(23.16)		
4a	89.8	45.9	2128	2443
	(276)	(276)		
5a	92.5	39.2	2121	2432
	(273)	(273)		
6a	88.5	45.2	2120	2443
	(282)	(282)		

[a] J values in Hz. J(P, P) values are given in parentheses. Spectra were run at 300 K and 32.4 MHz except for **3a** which was measured at 303 K and 121.5 MHz. The following solvents were used: CH_2Cl_2/MeOH (1:1) (**1**), CH_2Cl_2/MeOH/CH_3NO_2 (1:1:2) (**3**), CH_2Cl_2/CH_3NO_2 (3:2) (**5**), CH_2Cl_2 (**2**, **4**, **6**), CH_2Cl_2/CH_3NO_2 (2:1) (**1a**), CH_2Cl_2 (**2a**, **6a**), CH_2Cl_2-d_2/MeOH-d_4/CH_3NO_2-d_3 (1:1:1) (**3a**), CH_3NO_2 (**4a**), CH_2Cl_2/CH_3NO_2 (5:1) (**5a**). The given solvents and solvent mixtures also correspond to the general solubilities of the compounds. [b] ^3J(Pt, PPh) = 51 Hz.

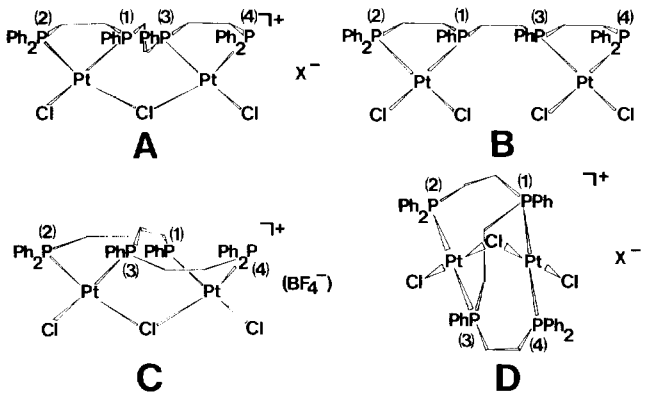

Scheme 2. Structure types observed in the dimers **1a–6a**. The (1)···(2) *cis* structure A occurs in the precursors of *cis,rac*- and *cis,meso*-[Pt_2Cl_4P4] (**1a** and **2a**), the (1)···(2) *cis* structure B in **1a** and **2a**, the(2)···(3) *cis* structure C in *rac*-[$Pt_2Cl_2(\mu$-Cl)-P4](BF$_4$) (**3a**), and the (2)···(3) *trans* structure D in *trans,meso*-[$Pt_2Cl_2(\mu$-Cl)P4](BF$_4$), *trans,rac*-[$Pt_2Cl_2(\mu$-Cl)P4](BPh$_4$), and *trans,meso*-[$Pt_2Cl_2(\mu$-Cl)P4](BPh$_4$) (**3a–6a**). Molecular modelling studies have shown that these structures are available without considerable strain.

92.9(2)°, respectively, and smaller than ideal *trans* angles of 178.0(3) and 175.2(3)°. Nevertheless, the Pt–Cl and Pt–P bond distances remain identical within the standard deviations. The chloride and phosphorus ligands surrounding a platinum atom occupy a plane. The platinum atom deviates 0.0377 Å from this plane towards the phenyl-ring of the PPh group. The so defined two planes of the molecule include an angle of 7.3°. The Pt–Pt distance is 6.338(1) Å.

A preliminary X-ray structure analysis of *cis,meso*-[Pt_2Cl_4P4] (**2a**) shows a very similar structure. Though the hydrogen positions have not been directly located it is convenient to make use of the *syn* and *anti* nomenclature previously described for comparable bimetallic oligophosphine complexes [14, 15]. In *cis,rac*-[Pt_2Cl_4P4] (**1a**) the hydrogen atoms of the central ethylene bridge show *syn,anti* conformation with respect to both platinum atoms, whereas *cis,meso*-[Pt_2Cl_4P4] (**2a**) is the *anti,anti* conformer. Nevertheless, the Pt–Pt distance remains nearly the same.

The occurrence of these conformers is partially a consequence of the different angular requirements of *rac* P4 (**1a**) and *meso* P4 (**2a**) coordinating two adjacent square-planar metal centers. Comparable differences have also been found in monomeric complexes containing P4 [16, 17]. However, since free rotation about the C–C bond of the central ethylene bridge is possible in **1a** and **2a** other rotation conformers may also occur. The observed structures are due to minimized free energies and crystallographic constraints. This is confirmed by the presence of short intramolecular contact approaches.

Though tetraphos-1 (P4) contains only ethylene bridges and phenyl-substituted phosphorus atoms, a comparison with binuclear complexes of two other oligophosphines possessing ethylene and central methylene bridges and phenyl- and ethyl-substituted phosphorus atoms seems reasonable. **1a** shows an open-mode structure where the two metal centers are well separated by 6.338(1) Å. In contrast to this [Pt_2Cl_2(eHTP)](PF$_6$)$_2$ (**7**), where eHTP is (Et_2PCH_2-

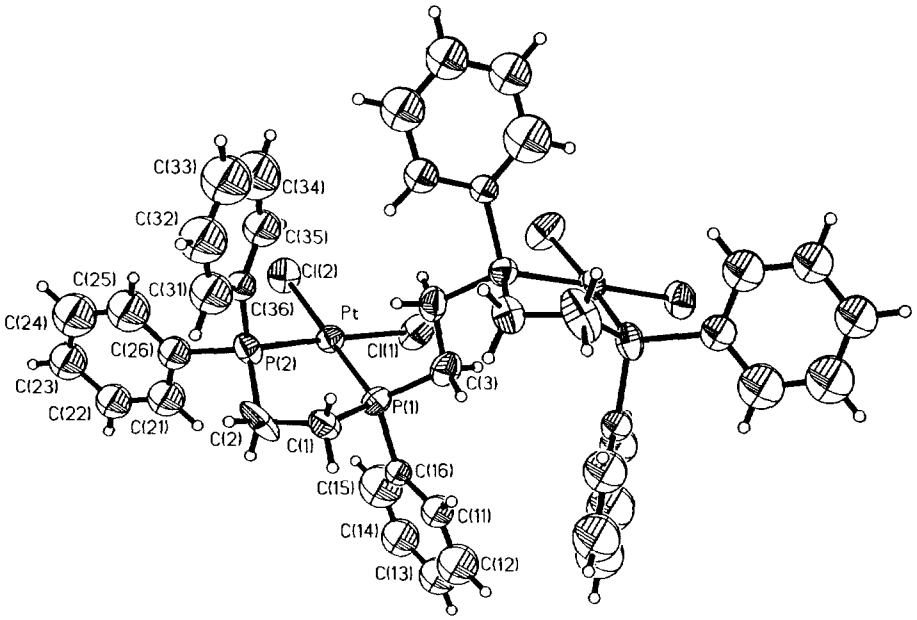

Fig. 1. View of *cis,rac*-[Pt_2Cl_4P4] (**1a**), showing the atomic numbering.

TABLE 4. Selected bond distances (Å) and bond angles (°) for *cis,rac*-[Pt_2Cl_4P4] (**1a**)

Pt–Cl(1)	2.347(7)	Pt–Cl(2)	2.359(7)
Pt–P(1)	2.212(6)	Pt–P(2)	2.222(7)
P(1)–C(1)	1.815(26)	P(1)–C(3)	1.787(26)
P(1)–C(16)	1.807(22)	P(2)–C(2)	1.818(25)
P(2)–C(26)	1.839(19)	P(2)–C(36)	1.834(21)
C(1)–C(2)	1.586(34)		
Cl(1)–Pt–Cl(2)	91.5(2)	Cl(1)–Pt–P(1)	89.1(2)
Cl(2)–Pt–P(1)	178.0(3)	Cl(1)–Pt–P(2)	175.2(3)
Cl(2)–Pt–P(2)	92.9(2)	P(1)–Pt–P(2)	86.5(3)
Pt–P(1)–C(1)	111.0(9)	Pt–P(1)–C(3)	112.3(10)
C(1)–P(1)–C(3)	102.8(13)	Pt–P(1)–C(16)	114.7(7)
C(1)–P(1)–C(16)	101.7(11)	C(3)–P(1)–C(16)	113.1(12)
Pt–P(2)–C(2)	107.9(8)	Pt–P(2)–C(26)	119.5(7)
C(2)–P(2)–C(26)	105.9(10)	Pt–P(2)–C(36)	110.4(7)
C(2)–P(2)–C(36)	107.0(10)	C(26)–P(2)–C(36)	105.5(9)
P(1)–C(1)–C(2)	109.2(17)	P(2)–C(2)–C(1)	109.0(17)
P(1)–C(3)–C(3A)	124.2(31)	P(1)–C(16)–C(11)	118.9(7)
P(1)–C(16)–C(15)	121.1(7)	P(2)–C(26)–C(21)	116.7(6)
P(2)–C(26)–C(25)	123.3(6)	P(2)–C(36)–C(31)	119.3(6)
P(2)–C(36)–C(35)	120.7(6)		

$CH_2)_2PCH_2P(CH_2CH_2PEt_2)_2$, approaches a closed-mode configuration with a Pt–Pt distance of 4.6707(9) Å [18]. The presence of this conformation is mainly attributed to the angular constraints imposed by the central methylene bridge and to increased intramolecular steric contacts due to chelate ring puckering differences.

For similar reasons *rac*-[Ni_2Cl_4(eLTTP)] (**8**) [14], where eLTTP is $(Et_2PCH_2CH_2)(Ph)PCH_2P(Ph)$-$(CH_2CH_2PEt_2)$, shows a Ni–Ni distance of 5.417(1) Å. However, *meso*-[Ni_2Cl_4(eLTTP)] (**9**) has a Ni–Ni distance of 6.272(1) Å, which only slightly differs from the Pt–Pt distance in **1a**. In order to properly assess the intramolecular steric effects, it is appropriate to compare the average M–P–CH_2 angles. In **7** this value is 121°, in **8** it is 118°, and in **1a** it is only 110°. In **9** the relaxation of one of these angles to 115° is attributed to a less crowded environment of one half of the complex. It seems likely that a reduction of these angles is in line with sterically less demanding configurations leading to longer M–M′ separations.

3–6 contain non-coordinating anions and therefore the incorporation of the counterion is not possible. Instead of it a rearrangement process leads to the *cis* structure C, which is in equilibrium with the *trans* structure D in *rac*-[$Pt_2Cl_2(\mu$-Cl)P4](BF_4) (**3a**) (see Scheme 2). In *trans,meso*-[$Pt_2Cl_2(\mu$-Cl)P4](BF_4), *trans,rac*-[$Pt_2Cl_2(\mu$-Cl)P4](BPh_4) and *trans,meso*-[$Pt_2Cl_2(\mu$-Cl)P4](BPh_4) (**4a–6a**) this rearrangement produces the *trans* structure type D.

The $^{31}P\{1H\}$ NMR spectral parameters of **3–6** and **3a–6a** are in agreement with the proposed structures (see Table 3). In **5** the PPh_2 signal is shifted to higher field and the ^1J(Pt, PPh_2) value is reduced to 688 Hz. This indicates dynamic PPh_2 groups. The presence of a small amount of dissociative PPh_2 populations at −13.0 ppm shows the occurrence of an equilibrium with a species containing a dissociative phosphine arm.

rac-[$Pt_2Cl_2(\mu$-Cl)P4](BF_4) (**3a**) shows an equilibrium between structures C and D. The ^2J(PPh, PPh_2) + ^3J(PPh, PPh_2) values are partially dynamically reduced and in the *cis* range [5, 19] in accordance with structure C. However, the occurrence of a large low-field shift of one PPh group is indicative for structure D and due

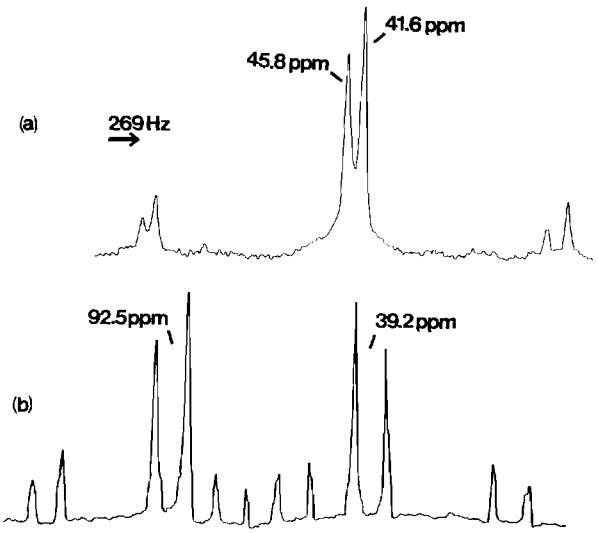

Fig. 2. $^{31}P\{^1H\}$ NMR spectra at 32.4 MHz and 300 K of: (a) a CH_2Cl_2/CH_3NO_2 (2:1) solution of *cis,rac*-$[Pt_2Cl_4P4]$ (**1a**), the spectrum is consistent with an A_2B_2 spin system; (b) a CH_2Cl_2/CH_3NO_2 (5:1) solution of *trans,rac*-$[Pt_2Cl_2(\mu\text{-}Cl)P4](BPh_4)$ (**5a**), the spectrum is consistent with an AA'–XX' spin system.

to the strong *cis* influence of the chloride ligand [12] in addition to the participation of each PPh group in two seven-rings [10]. The reduction of one ^1J(Pt, PPh_2) coupling to 1299 Hz confirms the presence of a dynamic process. A PPh group shows coupling to the second ^{195}Pt atom indicating the chloro bridge in **3a**. The ^3J(Pt, PPh) value of 51 Hz is comparable to earlier found ^3J(Pt, P) coupling constants [13].

trans,meso-$[Pt_2Cl_2(\mu\text{-}Cl)P4](BF_4)$, *trans,rac*-$[Pt_2Cl_2(\mu\text{-}Cl)P4](BPh_4)$ and *trans,meso*-$[Pt_2Cl_2(\mu\text{-}Cl)P4](BPh_4)$ (**4a–6a**) show the typical low-field shifts for the PPh groups in agreement with structure D. The ^{31}P NMR spectra are in accordance with AA'XX' spin patterns typical for a *trans* P4 arrangement [6, 20]. This structure is confirmed by the ^2J(PPh, PPh_2) values in the ^2J(P, P) *trans* range [6, 19, 21] (see Table 3).

Figure 2 demonstrates the influence of the non-coordinating anion (BPh_4^-) compared with Cl^-. Transformation of **1** leads to the *cis* structure *cis,rac*-$[Pt_2Cl_4P4]$ (**1a**) and an A_2B_2 spin system (Fig. 2(a)), whereas the *trans* structure *trans,rac*-$[Pt_2Cl_2(\mu\text{-}Cl)P4](BPh_4)$ (**5a**) and an AA'XX' spin system (Fig. 2(b)) is formed from **5**.

Discussion

It has been shown that tetraphos-1 (P4) is able to coordinate two metal centers in a *cis* as well as a *trans* manner. This is a very unusual behavior for binuclear oligophosphine complexes [14, 15, 18] and certainly a consequence of the already mentioned high flexibility of P4. It is an example for the interesting possibility of varying M–M' separations in P4 dimers.

In $[Ni_2Cl_2(eHTP)]X_2$ the Ni–Ni distance depends on the counterion X for $X = Cl^-$, (BF_4^-) and (PF_6^-) [15]. A similar effect also depending on the counterion could produce differences within the intermediate products **1–6**. In the cases where non-coordinating anions prevent the incorporation of the counterions this could lead to a different reactivity of P4 towards a change of coordination. As a consequence not only the *trans* structure D is observed but also an equilibrium between this structure and the *cis* structure C occurs.

$NaBH_4$ reduction of $[Pt_2Cl_3P4]X$ species, where X^- is a non-coordinating anion, results in a displacement of the chloride ligands by hydride [22]. The observation of large ^3J(Pt, P) values in these species indicate that the two platinum centers approach each other. This could result in closed-mode structures comparable to **7**. Further work on this is in progress.

Supplementary material

Tables of thermal parameters (1 page), bond lengths and bond angles (3 pages), torsion angles, H-atom coordinates, and non-bonded distances (3 pages), and structure factors (7 pages) are available from the author on request.

Acknowledgement

We thank Dr E. Hovestreydt for much help.

References

1 M. M. Taqui Khan and B. Swamy, *Inorg. Chem., 26* (1987) 178.
2 A. M. Bradford, R. J. Puddephatt, G. Douglas, L. Manojlovic-Muir and K. W. Muir, *Organometallics, 9* (1990) 1579.
3 R. S. Paonessa and W. C. Trogler, *Inorg. Chem., 22* (1983) 1038.
4 E. C. Constable, S. M. Elder, J. Healy, M. D. Ward and D. A. Tocher, *J. Am. Chem. Soc., 112* (1990) 4590.
5 P. Brüggeller, *Inorg. Chem., 29* (1990) 1742.
6 P. Brüggeller, *Inorg. Chim. Acta, 155* (1989) 45.
7 R. B. King and P. N. Kapoor, *Inorg. Chem., 11* (1972) 1524; U. Puttfarcken and D. Rehder, *J. Organomet. Chem., 185* (1980) 219; J. M. Brown and L. R. Canning, *J. Organomet. Chem., 267* (1984) 179; A. E. Stiegman, A. S. Goldman, C. E. Philbin and D. R. Tyler, *Inorg. Chem., 25* (1986) 2976.
8 A. C. T. North, D. C. Phillips and F. S. Mathews, *Acta Crystallogr., Sect. A, 24* (1968) 351.
9 G. M. Sheldrick, SHELXS86, in G. M. Sheldrick, C. Krüger and R. Goddard, (eds.), *Crystallographic Computing 3*, Oxford University Press, London, 1985, p. 175.

10 P. E. Garrou, *Chem. Rev., 81* (1981) 229.
11 R. J. Blau and J. H. Espenson, *Inorg. Chem., 25* (1986) 878.
12 K. D. Tau and D. W. Meek, *Inorg. Chem., 18* (1979) 3574.
13 R. Huis and C. Masters, *J. Chem. Soc., Dalton Trans.*, (1976) 1796.
14 S. A. Laneman, F. R. Fronczek and G. G. Stanley, *Inorg. Chem., 28* (1989) 1872.
15 S. E. Saum, S. A. Laneman and G. G. Stanley, *Inorg. Chem., 29* (1990) 5065.
16 A. V. Rivera, E. R. De Gil and B. Fontal, *Inorg. Chim. Acta, 98* (1985) 153.
17 P. Brüggeller and Th. Hübner, *Acta Crystallogr., Sect. C, 46* (1990) 388.
18 S. E. Saum and G. G. Stanley, *Polyhedron, 6* (1987) 1803.
19 D. L. DuBois and A. Miedaner, *J. Am. Chem. Soc., 109* (1987) 113.
20 M. T. Bautista, K. A. Earl, P. A. Maltby and R. H. Morris, *J. Am. Chem. Soc., 110* (1988) 4056.
21 A. Scrivanti, A. Berton, L. Toniolo and C. Botteghi, *J. Organomet. Chem., 314* (1986) 369.
22 P. Brüggeller, unpublished results.